The Eurasia Proceedings of Science, Technology, Engineering & Mathematics (EPSTEM)
ISSN: 2602-3199

**The Eurasia Proceedings of Science, Technology, Engineering & Mathematics (EPSTEM)**

**Volume 1, Pages 286-303**

**ICONTES2017: International Conference on Technology, Engineering and Science**

# FAILURE MODES OF CONTINUOUS REINFORCED CONCRETE T-BEAMS STRENGTHENED USING CFRP LAMINATES

Mohammad Mohie Eldin
Beni-Suef University

Ahmed M. Tarabia
Alexandria University

Rahma F. Hasson
Sirte University

**Abstract:** Strengthening, repairing and rehabilitation of existing structures are very important functions of the construction industry nowadays. Laminates made of Carbon Fiber Reinforced Polymers (CFRP) have proved an excellent behavior when used for the strengthening, repairing and rehabilitation of existing structures. When CFRP laminates are used to strengthen continuous reinforced concrete (RC) T-beams, they may be fixed either in the lower soffit of the beam in the hogging moment zone (HMZ); or in the upper surface of the beam, in the sagging moment zone (SMZ) in the vicinity of mid-supports. Three types of failure modes may occur in such structures; crushing of concrete, debonding between CFRP laminates and concrete surfaces, and rupture of CFRP laminates. Each failure mode is conducted according to a certain criterion which is a function of both mechanical properties of materials (concrete, reinforcement, CFRP, and adhesive) and dimensions of both RC beam and CFRP strengthening laminates. This paper explains the sequence of occurring of the different failure modes of RC continuous T-beams of two spans strengthened using CFRP laminates either in SMZ or in HMZ. The paper contains the main details of the finite element (FE) modeling process, behavior of the strengthened beams either in SMZ and HMZ and the explanation of the different mechanisms of the failure modes of the strengthened beams. Studied parameters include CFRP length, thickness, width and locations of CFRP laminate across the flange of the studied T-beams. Also, unstrengthened (control) beams were studied to compare the results with the strengthened ones for better understanding of the effect of CFRP strengthening upon the behavior of the studied T-beams. ANSYS which is a very powerful FE tool is used to create 3-D models of this study. It was found that CFRP dimensions are the principle factors that affect the type of the failure mode occurred in the strengthened beam. Rupture occurs, only when strengthening of the HMZ, if the CFRP stress reaches its maximum value (strength) by using very small CFRP thickness comparing with the corresponding length. Debonding of CFRP laminates occurs if shear stress, in the adhesive (contact) (bond layer) between the laminate and the concrete, reaches its maximum value. Crushing of concrete occurs as a final stage after yielding of steel reinforcement, formation of a plastic hinge, moment redistribution till the capacity of the beam is reached which means failure.

***Keywords:*** ANSYS, CFRP, failure, rc beam, t-beam

## Introduction

When RC beams are externally strengthened using bonded CFRP laminates, a significant increasing in their ultimate strength was obtained both experimentally and theoretically [1]. Adding to this, the appropriate configuration of both longitudinal and transverse reinforcement increases the possibility of moment redistribution in such beams [2]. CFRP laminates may consist of a number of layers which should not increase its optimum value. Increasing this number of layers increases both flexure and shear strength and capacity, but it decreases moment redistribution, ductility, and CFRP ultimate strains [3, 4 and 12]. One of the important notes considering the failure modes of strengthened RC beams is that covering the entire sagging or hogging moment



- Selection and peer-review under responsibility of the Organizing Committee of the conference

*Corresponding author: Mohammad Mohie Eldin- E-mail: mohammad_mohie_eldin@yahoo.com

zones with CFRP laminates did not prevent their peeling failure [3]. In continuous beams, debonding mechanisms are governed by both moment redistribution and shear forces [14]. Also, end anchorages of CFRP laminates were found as effective tools to enhance the response of continuous RC beams with high strength reinforcement [4]. Adding to these, it was concluded [5] that wrapping methods of CFRP laminates affect ductility, flexural strength, and energy absorption capacity of the strengthened beams. One of the important effects of CFRP strengthening is to restrict the rotation of plastic hinges at their locations. Also, CFRP strengthening allows the formation of additional plastic hinges in unstrengthened cross-sections [14]. Although the importance of RC T-beams, few researches about their strengthening using CFR laminates are available. When strengthening such beams in the hogging moment zone, the CFRP laminates will be fixed over the T-beam flange. It was concluded that changing the position of CFRP strengthening across the beam flange, in the hogging moment zone, is effective upon the overall behavior [10]. Adding to this, the authors verified the excelent validity of using ANSYS [13] as an accurate FE tool for modeling such structural systems. Also, a technique to strengthen the zone of hogging moment in a continuous T-beam using CFRP laminates taking the column constrains into consideration was presented [6]. Mohie Eldin et al [11] studied the effect of changing the strengthening CFRP length in the hogging moment zone upon the overall behavior of T-section continuous beams and put a criterion to calculate the optimum CFRP strengthening length and the corresponding anchorage length. Finally, the aim of this paper is to study and explain the occurrence of failure modes of continuous RC T-beams strengthened using CFRP laminates.

## Finite Element Modeling

### *Element Types*

Six types of finite elements are used for 3-D modeling of the tested beams, as follows:

- *SOLID65* is used for modeling concrete elements. Shear transfer coefficients of open-cracks and closed-cracks are taken as 0.1 and 0.9, respectively. Crushing capability was turned off to allow convergence of the models.
- SOLID45 is used for modeling of steel plates of loading and supporting. It is similar to SOLID65 but wthout crushing/cracking capabilities.
- *LINK180* is used for modeling steel reinforcement bars and stirrups.
- *SHELL181* is used for modeling CFRP laminates.
- *CONTA173* and *TARGE170* are used to represent the adhesive or contact (sliding, gap or penetration) between the two surfaces of CFRP laminate and RC beam, respectively. Finally, element size of ($50 \times 50 \times 50$ mm) was chosen according to a convergence study.

### 2.1 *Material Properties*

Table 1 shows the mechanical properties of concrete, steel reinforcement and CFRP laminates. Figure 1 shows the typical stress strain curves of concrete and CFRP, respectively, while steel is modeled using an elastoplastic curve.

Table 1. Mechanical properties of materials

| **Concrete (MPa)** | | | | **Steel Bras (MPa)** | | | **CFRP Laminates (MPa)** | | |
|---|---|---|---|---|---|---|---|---|---|
| $\grave{f}_c$ | $f_r$ | $E_c$ | **Poisson's Ratio** | $f_y$ | $E_s$ | **Poisson's Ratio** | $\sigma_{u-CFRP}$ | $E_{CFRP}$ | **Poisson's Ratio** |
| 30 | 3 | 26000 | 0.2 | 400 | 200000 | 0.3 | 3050 | 165000 | 0.33 |

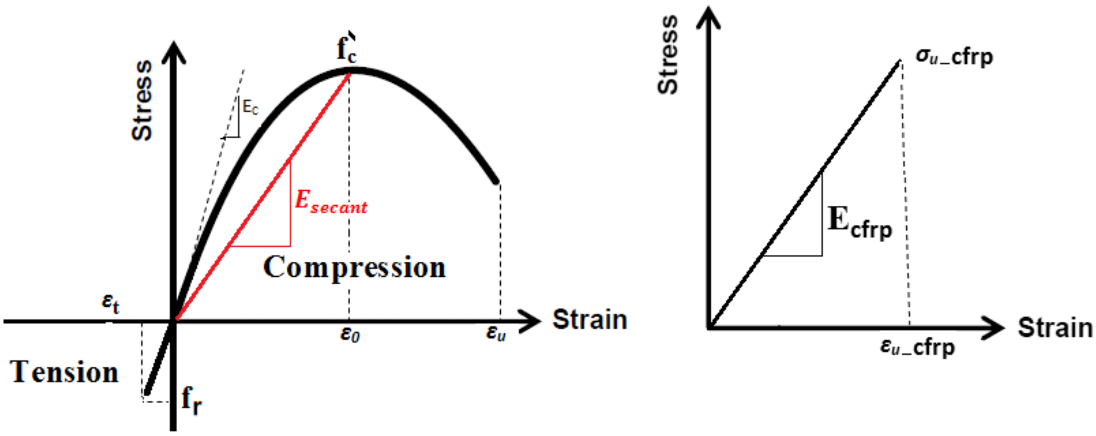


RC

(b) CFRP

Figure 1. Typical stress-strain curves

The adhesive material is modeled using a cohesive zone model (CZM) of six major parameters; maximum normal contact stress, critical fracture energy for normal separation, maximum equivalent tangential contact stress, critical fracture energy for tangential slip, artificial damping coefficient, and flag for tangential slip under compressive normal contact stress. Since debonding occurs due to shear failure, the first two parameters were not considered. The other four parameters are 6 N/mm$^2$, 0.75 N/mm, 0.1, and 1, according to an experimental bond-slip curve [7], as shown in Figure 2.

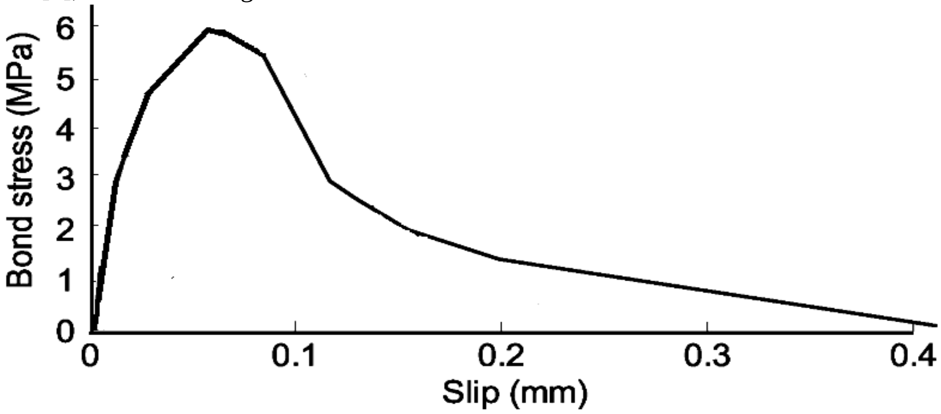


Figure 2. Local bond stress versus bond slip

*Dimensions of Modeled Beams*

Figures 3 and 4 show the dimensions, reinforcement, loading and CFRP patterns for strengthening of both hogging (HMZ) and sagging (SMZ) moment zones, respectively, of the modeled beam while Figure 5 shows the corresponding bending moment diagram. ECP-203 [18] was used to design the reinforcement of the T-beam which was 4-bars-**ϕ**24mm for the upper reinforcement in the HMZ and 4-bars-**ϕ**18mm as lower reinforcement in the SMZ. This beam is called BC1. To allow good investigation of the effect of CFRP strengthening, the designed reinforcement was reduced as follows:

1. When strengthening of HMZ, upper reinforcement was reduced by 75% from 4-bars-**ϕ**24mm to 4-bars-**ϕ**12mm, as shown in Figure 3.
2. When strengthening of SMZ, lower reinforcement was reduced by 55.6% from 4-bars-**ϕ**18mm to 4-bars-**ϕ**12mm, as shown in Figure 4.

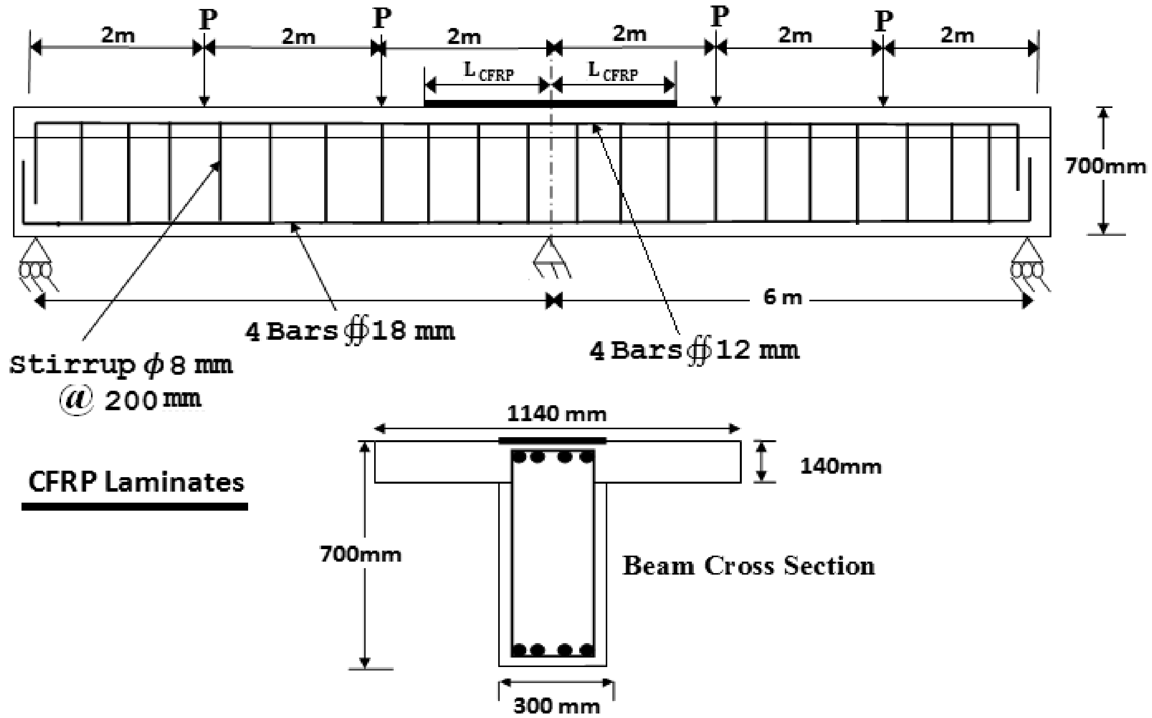


Figure 3. Dimensions, reinforcement and CFRP laminates in HMZ

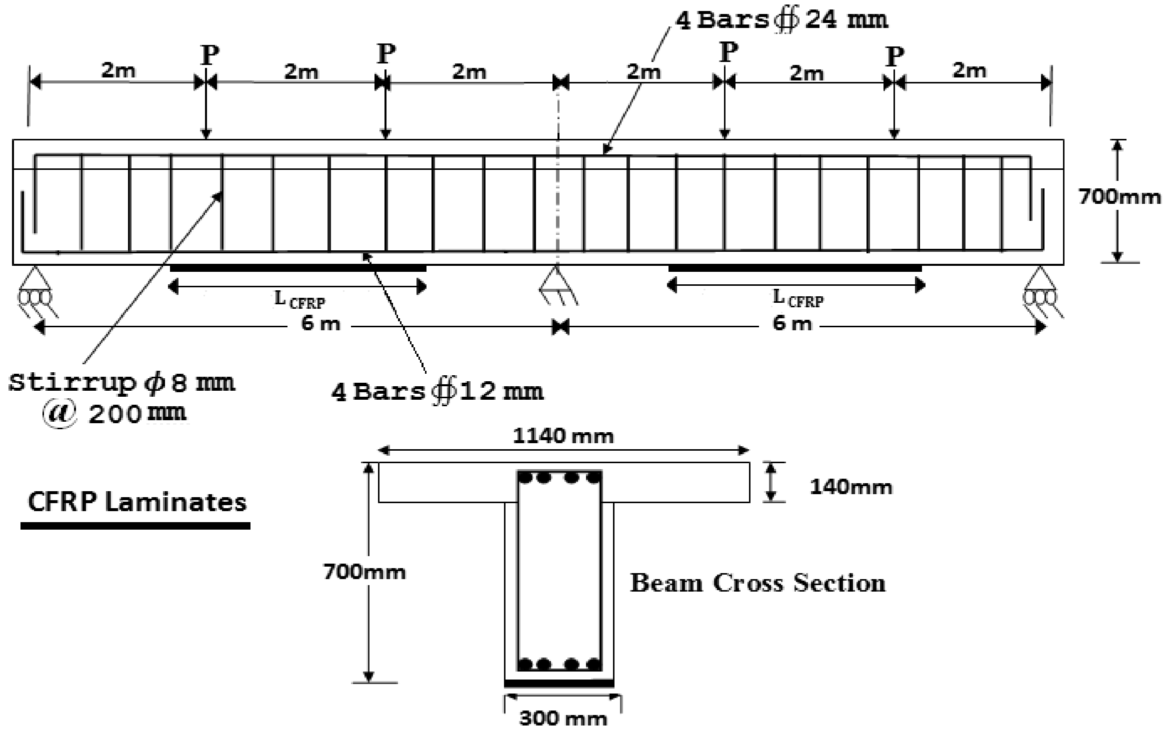


Figure 4. Dimensions, reinforcement and CFRP laminates in SMZ

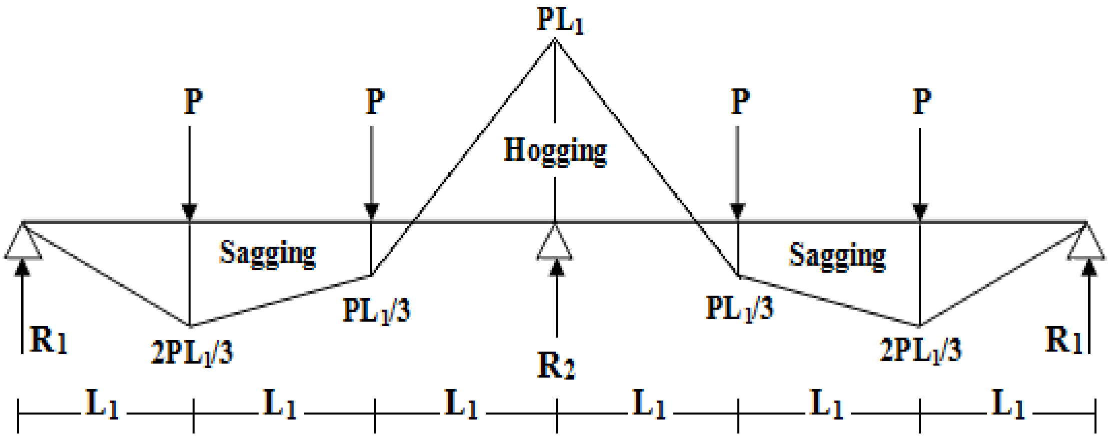

Figure 5. Bending moment diagram of the modeled beam

The thicknesses of CFRP strengthening laminates are designed using ECP-208 [19] for the T-beams with the reduced reinforcement to recover their original moment capacities either hogging or sagging. For strengthening of HMZ, CFRP thickness was designed and approximated to 0.9 mm. On the other hand, when strengthening of SMZ, CFRP thickness was designed for a rectangular beam (300×700mm) not for the T-beam to eliminate the effect of the T-beam flange which will cause the required CFRP thickness very small. As a result, CFRP thickness in the SMZ was approximated to 0.4 mm. CFRP laminate has width equals to the web width (300 mm) and its length equals ($2L_{CFRP}$) where ($L_{CFRP}$) is the CFRP strengthening length per span. In the SMZ, the laminates are fixed to the soffit of the beam web. However for HMZ, CFRP laminates are fixed in different positions across the beam flange, as shown in Figure 6.

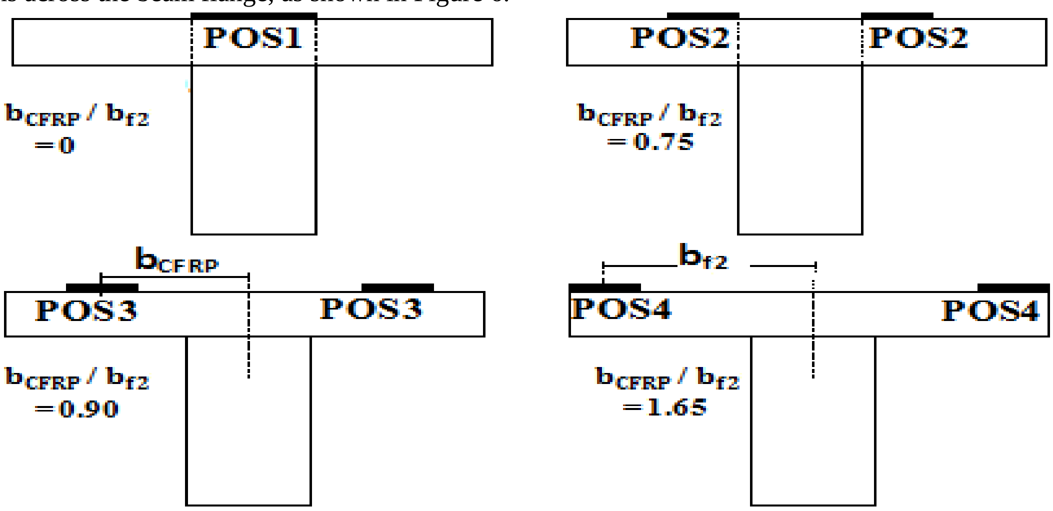

Figure 6. Positions of laminates in the HMZ across the beam flange

**Parameters of Studied Modeled Beams**

Four parameters are studied to investigate the mechanisms of the failure in the RC T-beams strengthened using CFRP laminates either in the SMZ or HMZ; length, thickness (Thick), width and locations (Loc) of CFRP laminate. Studied beams are divided into eight groups; 6 for HMZ and 2 for SMZ. Each of these groups was designed to study one parameter or one value of a parameter, while the other parameters are kept constant. The total number of studied beams is 35; 23 for HMZ including two rectangular beams as will be shown later and 12 for SMZ. For HMZ, main dimensions are 0.9mm for thickness, 600mm for short laminate and 1200mm for long laminate while the laminates are fixed above the web.

For SMZ, main dimensions are 0.4mm for thickness, 4000mm for length while the laminates are fixed to the soffit of the web. Tables 2 and 3 show the details of these groups for strengthening of HMZ and SMZ, respectively.

Table 2. Details of analyzed beams for parametric study of CFRP strengthening of HMZ

| Group | Parameter | Beam Code and Values of Parameters (Dimensions in mm) | | | | | | |
|---|---|---|---|---|---|---|---|---|
| **(0)** | **---------** | **Beam Code** | BC1 | It is the Original Unstrengthened (Control) Beam | | | | |
| **(1)** | **Length** | **Beam Code** | BS1 | BS2 | BS3 | BS4 | BS5 | BS6 |
| | | **Length** | 400 | 600 | 900 | 1100 | 1200 | 1500 |
| **(2)** | **Thickness (Length = 600mm)** | **Code** | BS7 | BS8 | BS2 | BS9 | --- | --- |
| | | **Thickness** | 0.2 | 0.5 | 0.9 | 1.8 | --- | --- |
| **(3)** | **Thickness (Length = 1200mm)** | **Beam Code** | BS10 | BS11 | BS5 | BS12 | BS13 | --- |
| | | **Thickness** | 0.2 | 0.5 | 0.9 | 1.8 | 3.6 | --- |
| **(4)** | **Width (Length = 1200mm)** | **Beam Code** | BS14 | BS15 | BS5 | --- | --- | --- |
| | | **Width** | 100 | 200 | 300 | --- | --- | --- |
| **(5)** | **Location (Length = 600mm)** | **Beam Code** | BS2 | BS16 | BS17 | BS18 | --- | --- |
| | | **Location** | POS1 | POS | POS3 | POS4 | --- | --- |
| **(6)** | **Location (Length = 1200mm)** | **Beam Code** | BS5 | BS19 | BS20 | BS21 | --- | --- |
| | | **Location** | POS1 | POS | POS3 | POS4 | | |

Table 3. Details of analyzed beams for parametric study of CFRP strengthening of SMZ

| Group | Parameter | Beam Code and Values of Parameters (Dimensions in mm) | | | | | | | | |
|---|---|---|---|---|---|---|---|---|---|---|
| **(0)** | **---------** | **Code** | BC1+ | It is the Original Unstrengthened (Control) Beam | | | | | | |
| **(7)** | **Length** | **Code** | BS1+ | BS2+ | BS3+ | BS4+ | BS5+ | BS6+ | BS7+ | BS8+ |
| | | **Length** | 800 | 1000 | 2000 | 3000 | 3800 | 4000 | 4100 | 4300 |
| **(8)** | **Thickness** | **Code** | BS9+ | BS10+ | BS6+ | BS11+ | BS12+ | --- | --- | --- |
| | | **Thick.** | 0.1 | 0.2 | 0.4 | 0.6 | 0.8 | --- | --- | --- |

**Strengthening of HMZ**

*Effect of CFRP Length*

Figure 7 shows the distribution of shear stresses in the bond layer between beam and CFRP along the length of the laminates. Increasing the length leads to decreasing of the bond stresses. This means that the probability of debonding decreases with increasing of CFRP length. Table 4 shows modes of failure for the different lengths of CFRP strengthening which insures this result.

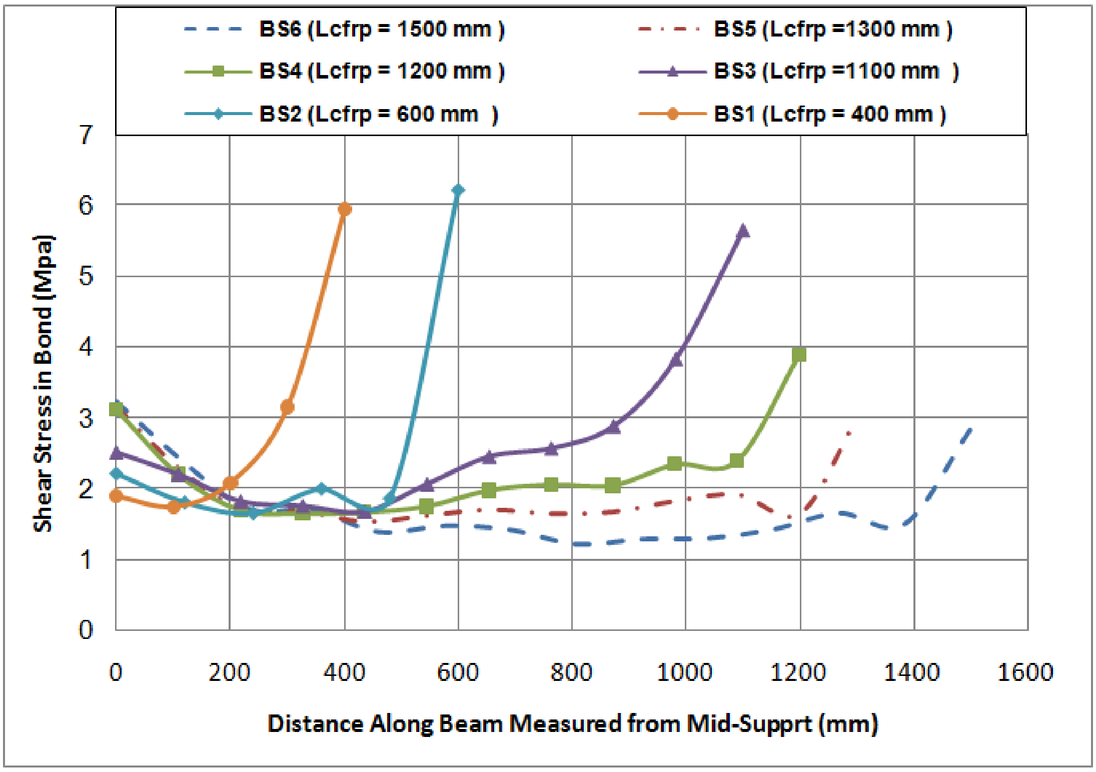


Figure 7. Shear stress in bond layer for different CFRP lengths

Table 4. Failure modes according to change of CFRP length

| **Beam Code** | BS1 | BS2 | BS3 | BS4 | BS5 | BS6 | BC1 |
|---|---|---|---|---|---|---|---|
| **CFRP Length (mm)** | 400 | 600 | 900 | 1100 | 1200 | 1500 | 0.0 |
| **Failure Mode** | CFRP Debonding | | | | Concrete Crushing at Mid-Support | | |

*Optimum (Effective) Length*

The optimum length is the length beyond it no improvement in the behavior of the strengthened beam is achieved. According to the results, it is the minimum length which does not allow the debonding of the CFRP laminate, and hence the failure mode will be only according to the failure of the concrete. Additional condition is that after the optimum length, no (significant) increasing in both the ultimate loading and the maximum deflection has to be noticed.

*Effect of CFRP Thickness*

Figures 8 and 9 show the distribution of shear stresses in the bond layer (contact) (epoxy) between the concrete surface and the CFRP laminates for CFRP lengths 600mm (short) and 1200mm (long), respectively. The stresses at the end of the CFRP laminates exceed the maximum shear stress which is 6Mpa for two thicknesses (0.9 and 1.8mm) and (1.8 and 3.6mm) for CFRP lengths 600mm and 1200mm, respectively. This means the occurrence of debonding at these two thicknesses of each length. Figures 10 and 11 show the stresses in CFRP laminates at failure for both short and long CFRP lengths, respectively.

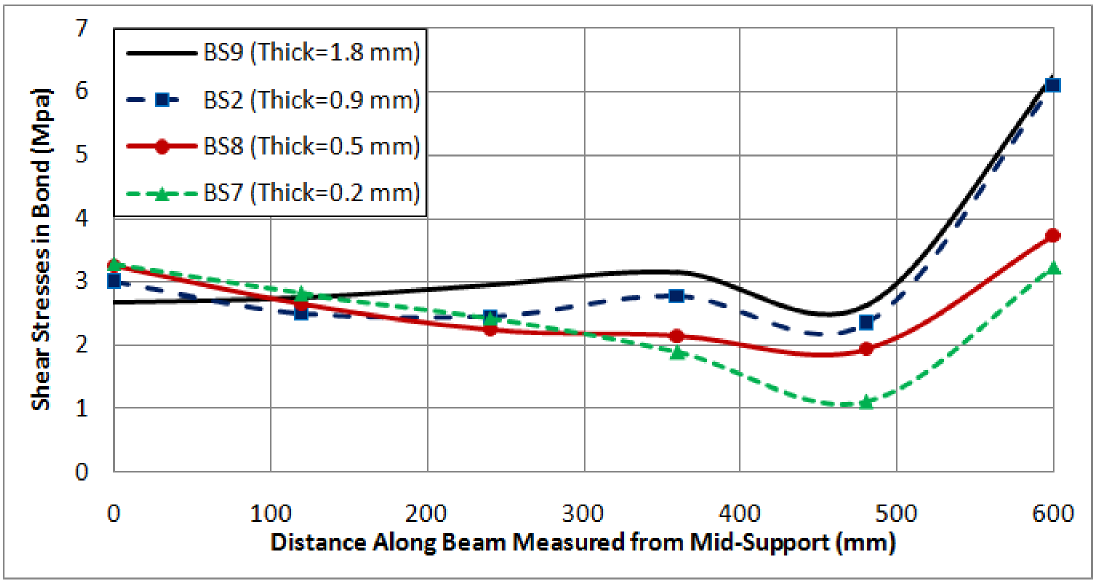


Figure 8. Shear bond stresses along CFRP length of 600mm for different thicknesses

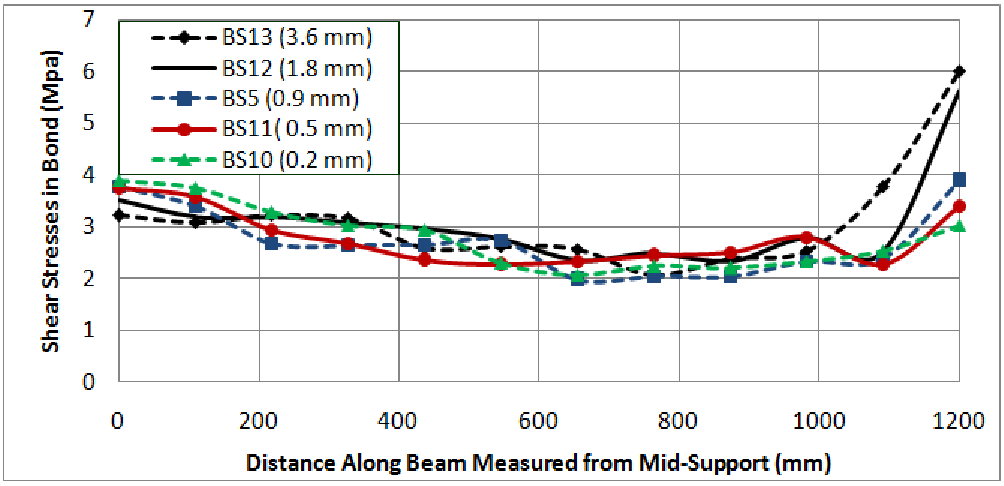


Figure 9. Shear bond stresses along CFRP length of 1200mm for different thicknesses

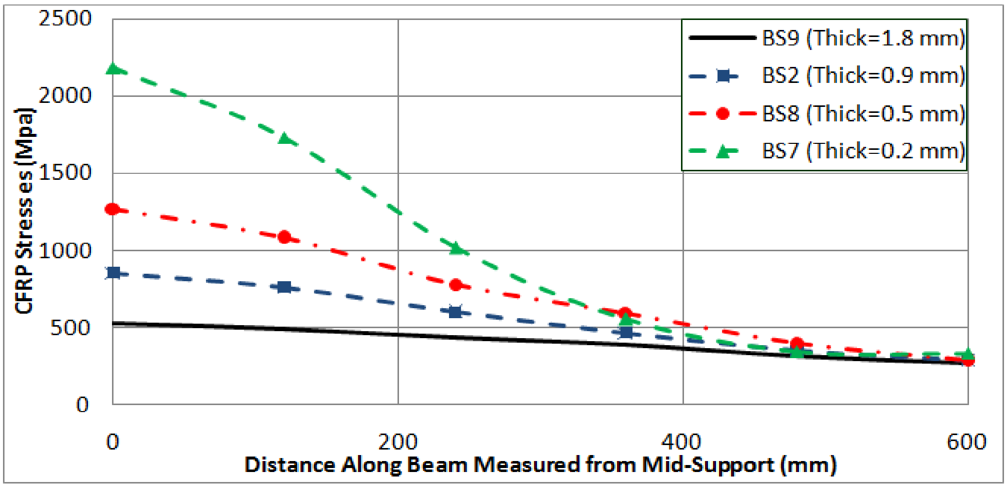


Figure 10. CFRP stresses at failure for short CFRP length

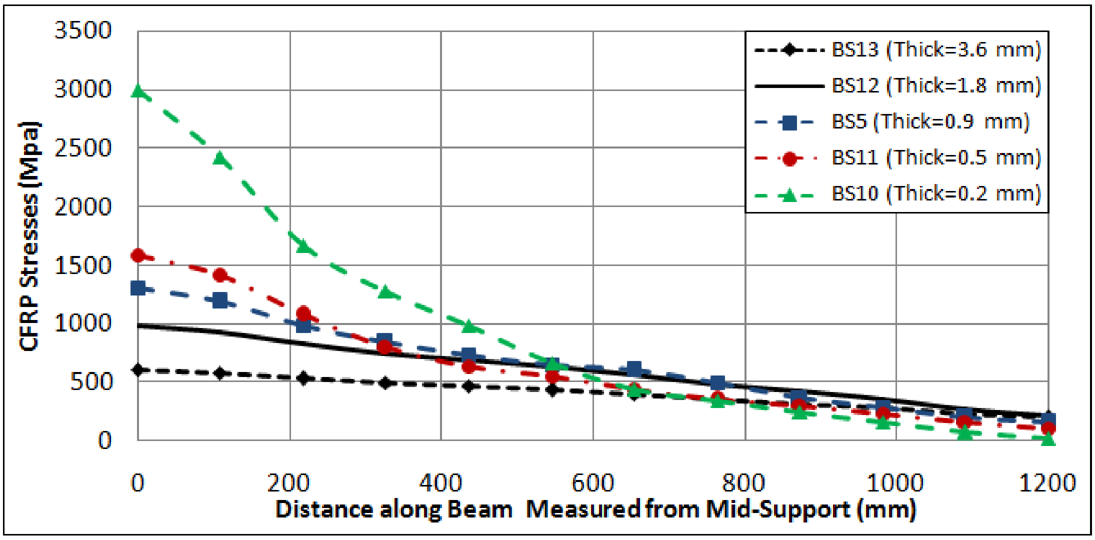


Figure 11. CFRP stresses at failure for long CFRP length

CFRP stresses for 0.2mm-thickness of long CFRP length reaches the maximum value which is 3050 MPa, as shown in Figure 11. However, this does not occur in the short CFRP laminate of the same thickness, as shown in Figure 10. The explanation is that CFRP thickness is very small, especially when compared to its length. This type of failure is called "rupture". Table 5 shows failure modes of different thicknesses of each length. It can be concluded that increasing CFRP thickness beyond a certain value or limit will cause debonding failure which is not recommended since it is considered as a brittle failure.

Table 5. Failure modes of different thicknesses for variable lengths

| | **CFRP Length = 600mm** | | | | **CFRP Length = 1200mm** | | | | |
|---|---|---|---|---|---|---|---|---|---|
| **Code** | BS7 | BS8 | BS2 | BS9 | BS10 | BS11 | BS5 | BS12 | BS13 |
| **Thick. (mm)** | 0.2 | 0.5 | 0.9 | 1.8 | 0.2 | 0.5 | 0.9 | 1.8 | 3.6 |
| **Failure Mode** | Concrete Crushing at Mid-Support | | CFRP Debonding | | CFRP Rupture | Concrete Crushing at Mid-Support | | CFRP Debonding | |

*Maximum CFRP Thickness*

According to the previous results, the allowable CFRP thickness can be defined as the maximum thickness that does not allow debonding failure.

*Effect of CFRP Width*

Table 6 shows modes of failure for the different studied widths of CFRP laminates.As shown, all beams failed by crushing of concrete at mid-support. This means that widths of CFRP laminates have no effect upon the behavior of the strengthened T-beams.

Table 6. Failure modes of different locations for variable lengths

| **Beam Code** | BS14 | BS15 | BS5 | BS18 |
|---|---|---|---|---|
| **Width (mm)** | 100 | 200 | 300 | POS4 |
| **Failure Mode** | Concrete Crushing at Mid-Support | | | |

*Effect of CFRP Location*

Table 7 shows the modes of failure for the different locations of CFRP laminate across the flange for both short and long CFRP lengths. As shown, the location does not affect the modes of failure.

Table 7. Failure modes of different locations for variable lengths

| | **CFRP Length = 600mm** | | | | **CFRP Length = 1200mm** | | | |
|---|---|---|---|---|---|---|---|---|
| **Beam Code** | BS2 | BS16 | BS17 | BS18 | BS5 | BS19 | BS20 | BS21 |
| **Position** | POS1 | POS2 | POS3 | POS4 | POS1 | POS2 | POS3 | POS4 |
| **Failure Mode** | CFRP Debonding | | | | Concrete Crushing at Mid-Support | | | |

*Failure Modes*

Three failure modes were recognized for the studied strengthened beams in HMZ, as follows:

i. Crushing of the concrete.
ii. Debonding between CFRP laminate and concrete surface.
iii. Rupture of the CFRP laminate.

*Crushing Failure Mode*

Crushing failure in concrete was found to occur only at the mid-support. To check and confirm this observation, a T-section beam was compared with two rectangular beams; one is an unstrengthened (control) beam while the second is a strengthened beam. The rectangular section has the same depth as the T-section and a width equals width of the T-beam web. Figures 12 and 13 show the relation between the applied load and its corresponding moment at both mid-support and span, respectively, for control (unstrengthened) beams. Figures 14 and 15 show the same relation at both mid-support and span, respectively, for strengthened beams.

*Control Beams*

As shown in Figure 12, the negative (hogging or mid-support) moment at first crack for the T-section beam is much more that for the rectangular beam. After its first crack and due to both propagation of cracks and low reinforcement ratio, the hogging (negative) moment of T-beam decreases dramatically, with a very slight increase in the applied load, and it follows a behavior path very close to that of the rectangular beam. According to Figure 12, a horizontal plateau exists after the yielding of upper steel reinforcement for both rectangular and T-section beams. This means a formation of a plastic hinge at mid-support zone. After this and due to the redistribution of moments, the span (sagging) (positive) moment will exceed with loading till failure, as shown in Figure 13. Rectangular beam failed in span while T-beam failed at mid-support. This means that the failure of T-section beam at mid-support is according to the presence of its flange.

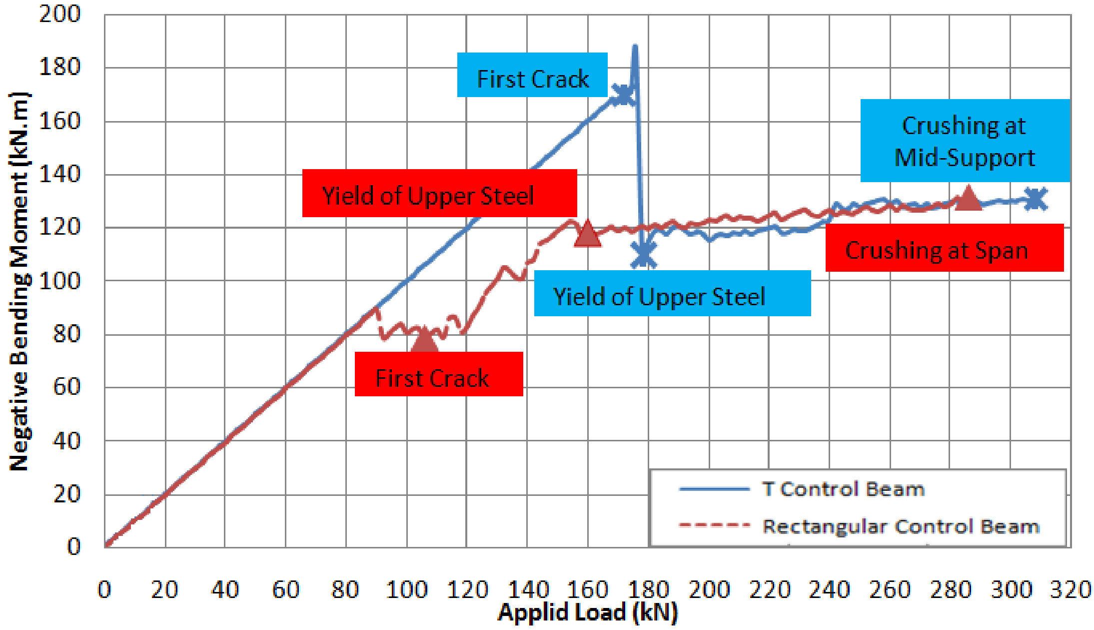


Figure 12. Mid-support moment versus applied loading for control beams

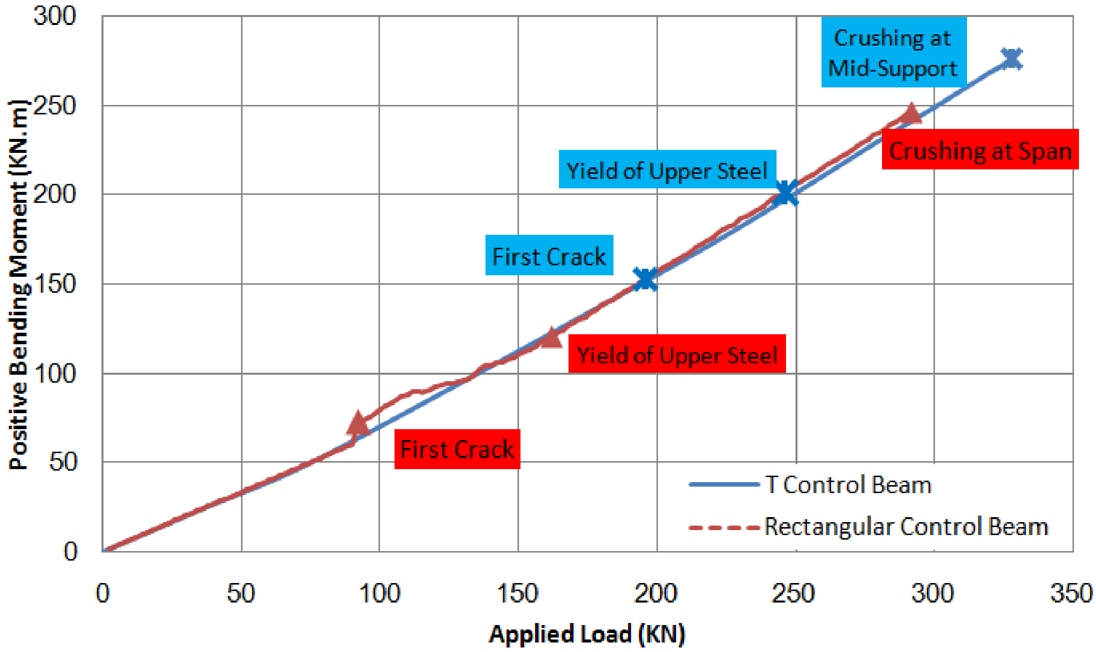


Figure 13. Maximum span moment versus applied loading for control beams

*Strengthened Beams*

According to Figure 14, upper reinforcement yielded first due to the presence of CFRP laminate. After that, lower reinforcement yielded. As shown in Figure 15, after the yielding of the lower reinforcement, a small horizontal plateau exists. This means a formation of a plastic hinge at the zone of maximum-span-moment due to the presence of CFRP strengthening. According to the redistribution of the moments, the moment at the mid-support will exceed with loading till failure. Again, rectangular beam failed in span while the T-beam failed at mid-support.

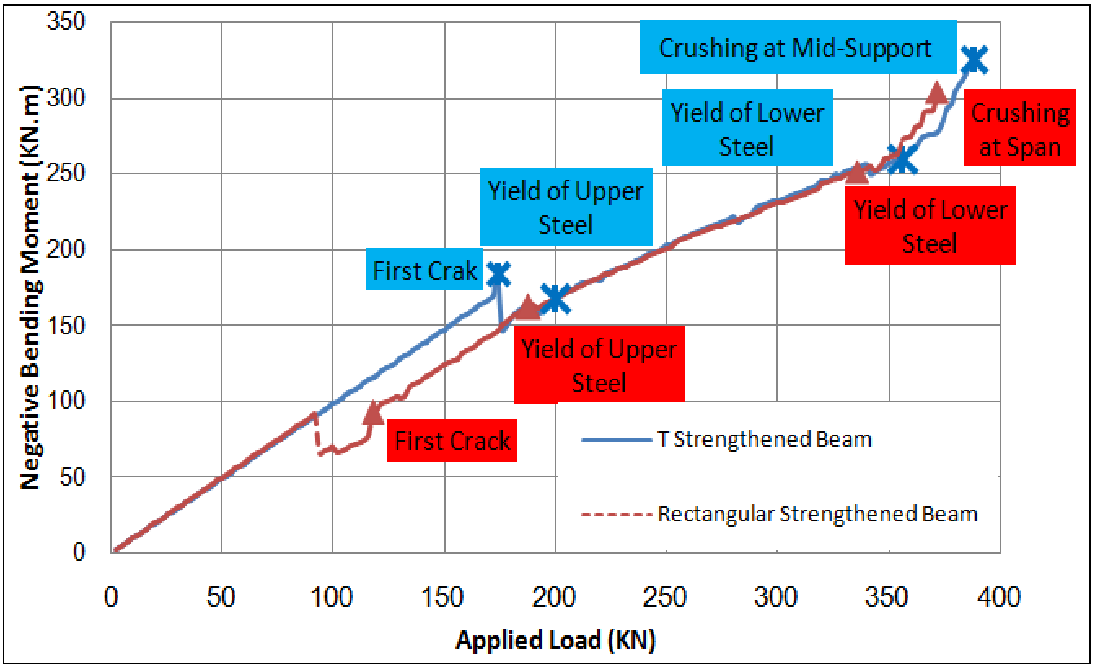


Figure 14. Mid-support moment versus applied loading for strengthened beams

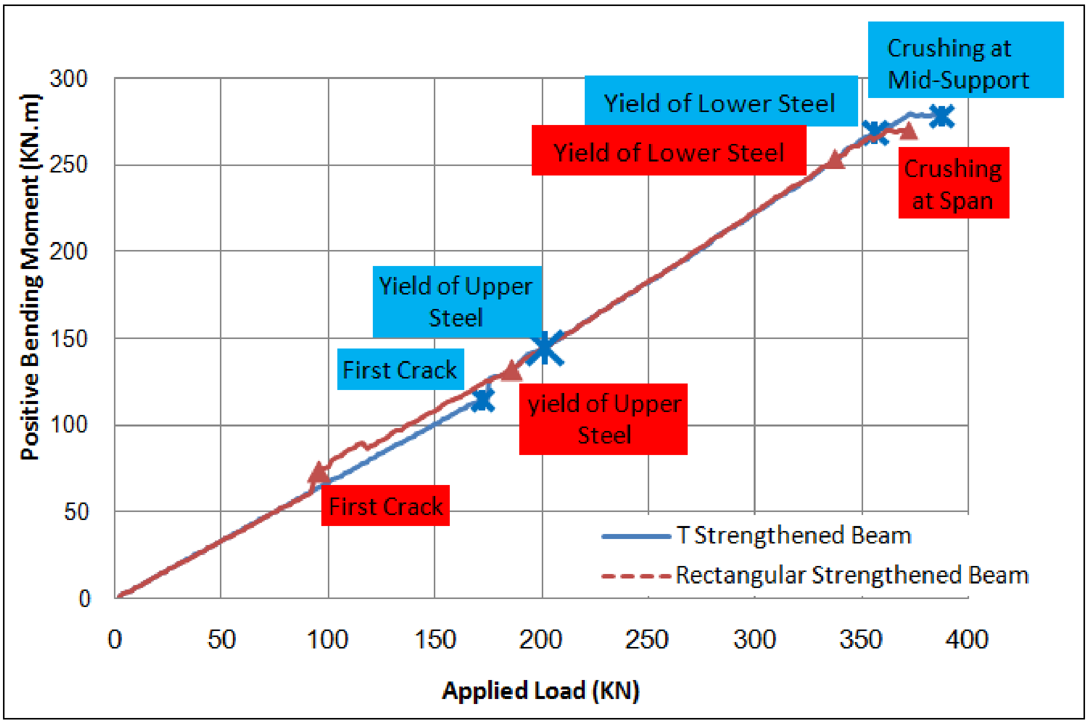


Figure 15. Maximum span moment versus applied loading for strengthened beams

*Debonding Failure Mode*

As illustrated and discussed before, debonding failure mode occurs if the stresses of CFRP laminates exceed the maximum shear stress of the bond layer (adhesive) between the CFRP laminate and the concrete beam. The probability of debonding decreases with decreasing of CFRP length and increasing of CFRP thickness.

*Rupture Failure Mode*

This type of failure, as mentioned before, occurs when the stresses of CFRP laminate reaches its maximum value. The only reason of rupture is to use very small CFRP thickness compared with CFRP length.

*Failure Mechanisms*

Steps of forming a failure mechanism with continuing of applying loads are as follows:

i. The upper reinforcement at the mid-support reaches the yield.

ii. Due to the presence of the CFRP, no plastic hinge will form in the mid-support region (at the upper reinforcement).

iii. The lower reinforcement in the span reaches yield.

iv. A plastic hinge is formed in the location of the maximum positive moment.

v. Moment redistribution between positive and negative moments begins.

vi. Negative moment increases till failure which will occur in one of the three ways:

   a) For long CFRP laminates (or for small CFRP thickness), the failure mode is concrete crushing at mid-support.
   b) For short CFRP laminates (or for large CFRP thickness), the failure mode is debonding between CFRP laminates and concrete surface.
   c) For long CFRP laminate with a very small thickness, comparing with the length, the failure mode is rupture of the CFRP laminate.

**Strengthening of SMZ**

*Effect of CFRP Length*

Figure 16 shows the distribution of shear stresses in the bond layer between beam surface and CFRP laminates along their lengths. Increasing the length leads to decreasing of the bond stresses at the ends of the laminates. This means that the probability of debonding decreases with increasing of CFRP length. Table 8 shows modes of failure for different lengths of CFRP strengthening which insures this result.

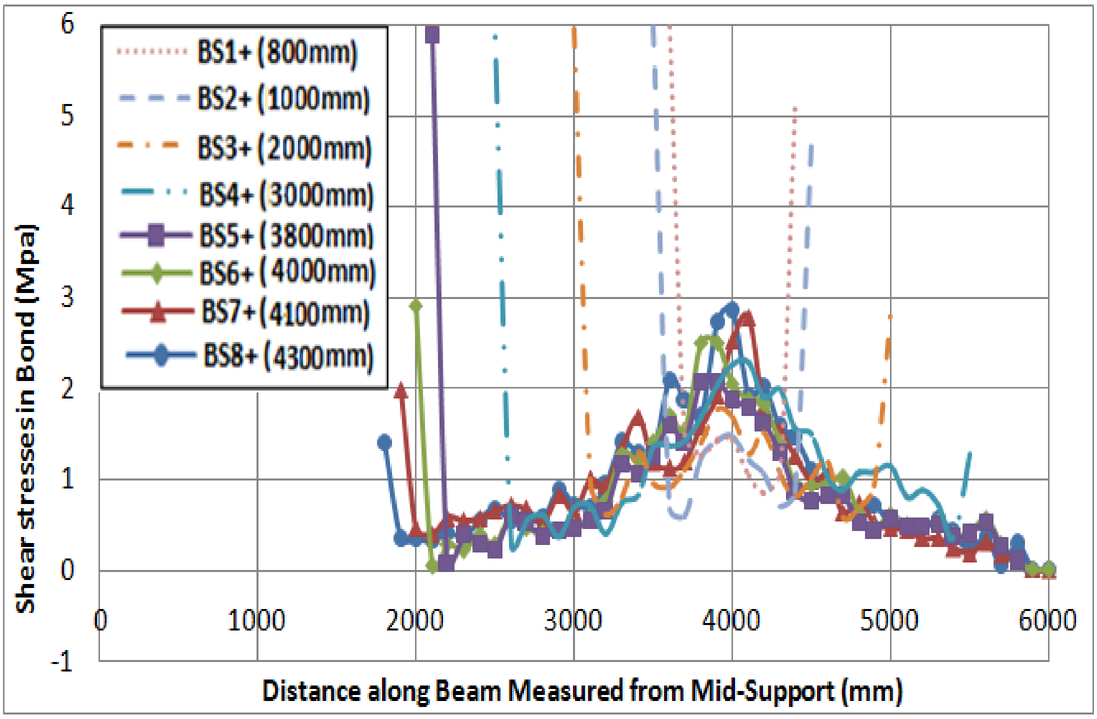


Figure 16. Shear stress in bond layer for different CFRP lengths

Table 8. Failure modes

| Beam Code | BS1+ | BS2+ | BS3+ | BS4+ | BS5+ | BS6+ | BS7+ | BS8+ |
|---|---|---|---|---|---|---|---|---|
| **CFRP Length (mm)** | 800 | 1000 | 2000 | 3000 | 3800 | 4000 | 4100 | 4300 |
| **Failure Mode** | CFRP Debonding | | | | | Concrete Crushing at Mid-Support | | |

*Optimum (Effective) Length*

According to the results, effective length is the length which does not allow the debonding of the CFRP laminate, and hence the failure mode will be only according to the failure of the concrete. Additional condition is that after the optimum length, no (significant) increasing in both the ultimate loading and the maximum deflection has to be noticed.

*Effect of CFRP Thickness*

Figure 17 shows the distribution of shear stresses in the bond layer between beam surface and CFRP laminates along their lengths. Increasing the thickness leads to increasing of the bond stresses at the ends of the laminates. This means that the probability of debonding increases with increasing of CFRP thickness. Table 9 shows modes of failure for different thicknesses of CFRP strengthening which insures this result.

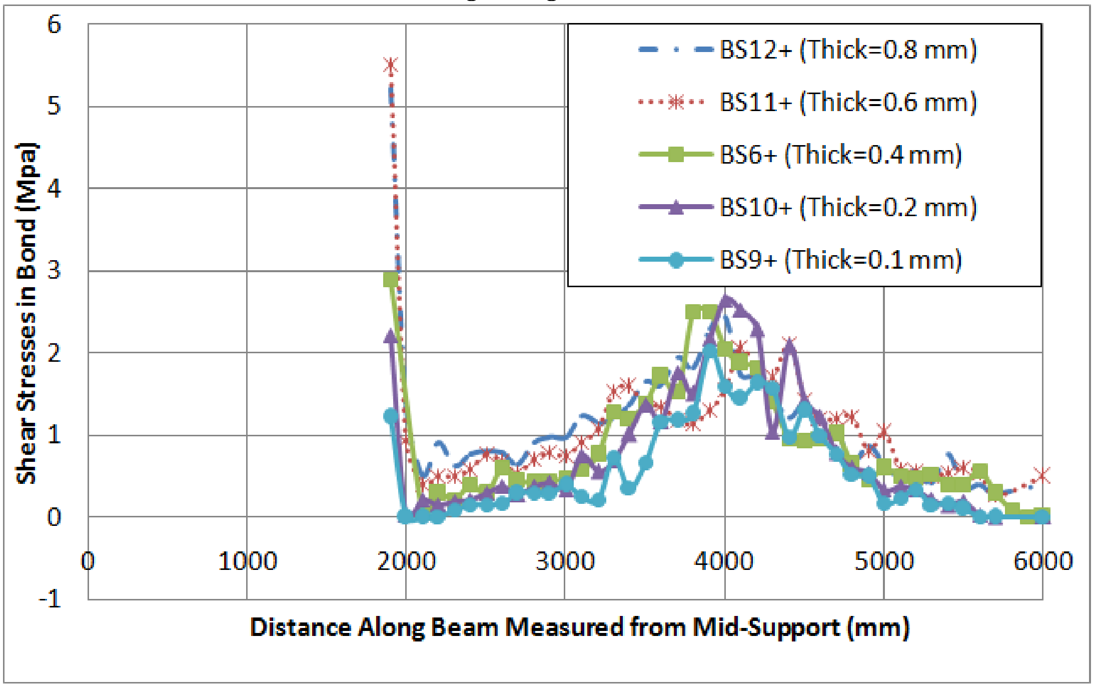


Figure 17. Shear stress in bond layer for different CFRP thicknesses

Table 9. Failure modes

| **Beam Code** | BS9+ | BS10+ | BS6+ | BS11+ | BS12+ |
|---|---|---|---|---|---|
| **CFRP Thickness (mm)** | 0.1 | 0.2 | 0.4 | 0.6 | 0.8 |
| **Failure Mode** | Concrete Crushing at Mid-Support | | | CFRP Debonding | |

*Maximum CFRP Thickness*

It is the maximum thickness that does not allow debonding failure.

*Failure Modes*

*Crushing Failure Mode*

Figures 18 and 19 show the relation between the applied load and the corresponding moment at both mid-support and span, respectively, for the control (unstrengthened) beam (BC1+), while Figures 20 and 21 show the same relations for the strengthened beam (BS6+).

*Control Beams*

According to Figures 18 and 19, stages of behavior till failure are as follows:

a. Lower steel starts to yield.

b. Formation of a plastic hinge in the span.
c. The positive (sagging) (span) moment increases slightly and the negative moment increases obviously.
d. Upper steel (at mid-support) starts to yield.
e. Crushing of concrete at mid-support.

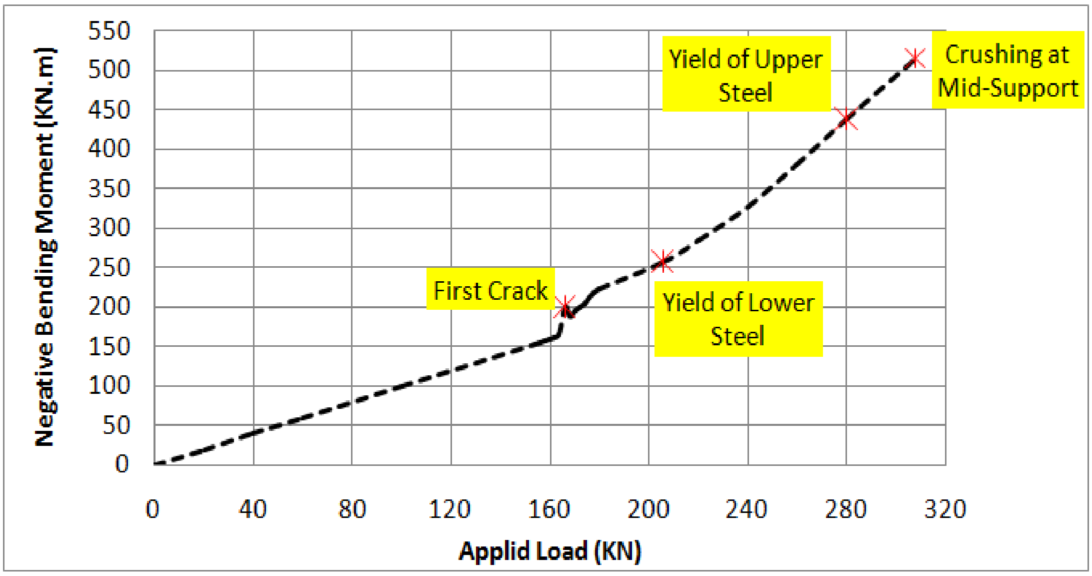


Figure 18. Mid-support moment versus applied loading for control beam

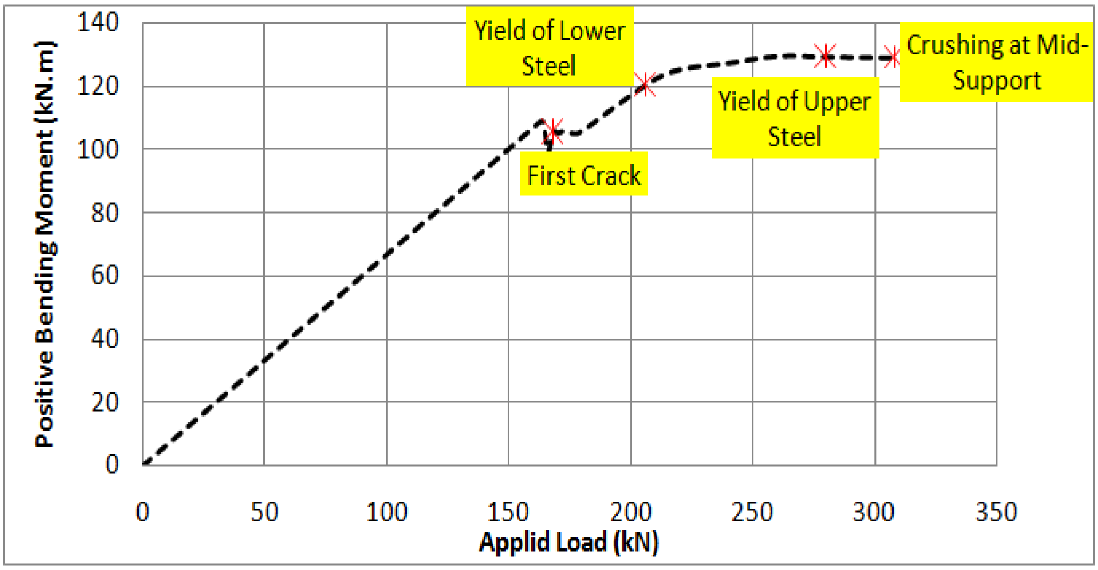


Figure 19. Maximum span moment versus applied loading for control beam

*Strengthened Beams*

According to Figures 20 and 21, the stages of behavior till failure are as follows:

a. Lower steel starts to yield.
b. No plastic hinges in the span due to the presence of the CFRP.
c. No crushing in the span due to the large dimensions of the flange.
d. Upper steel (at mid-support) starts to yield.
e. Formation of a plastic hinge at the mid-support.
f. The negative (hogging) (mid-support) moment increases slightly and the positive moment increases obviously.
g. Crushing of concrete at mid-support, since the compression zone is a part of a rectangular section, while it is a part of T-section in the span.

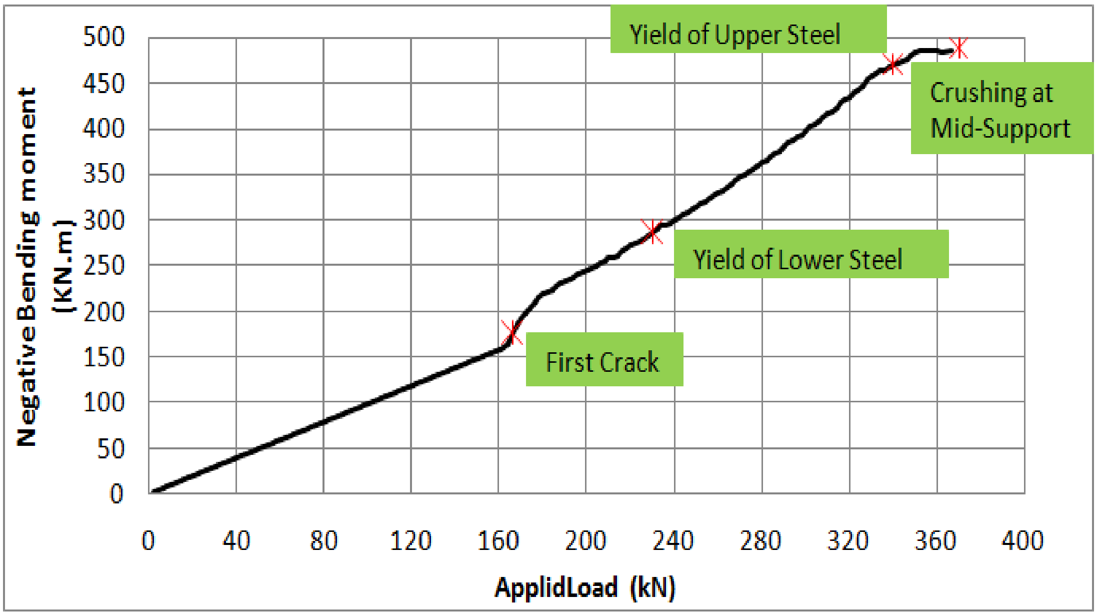


Figure 20. Mid-support moment versus applied loading for strengthened beam

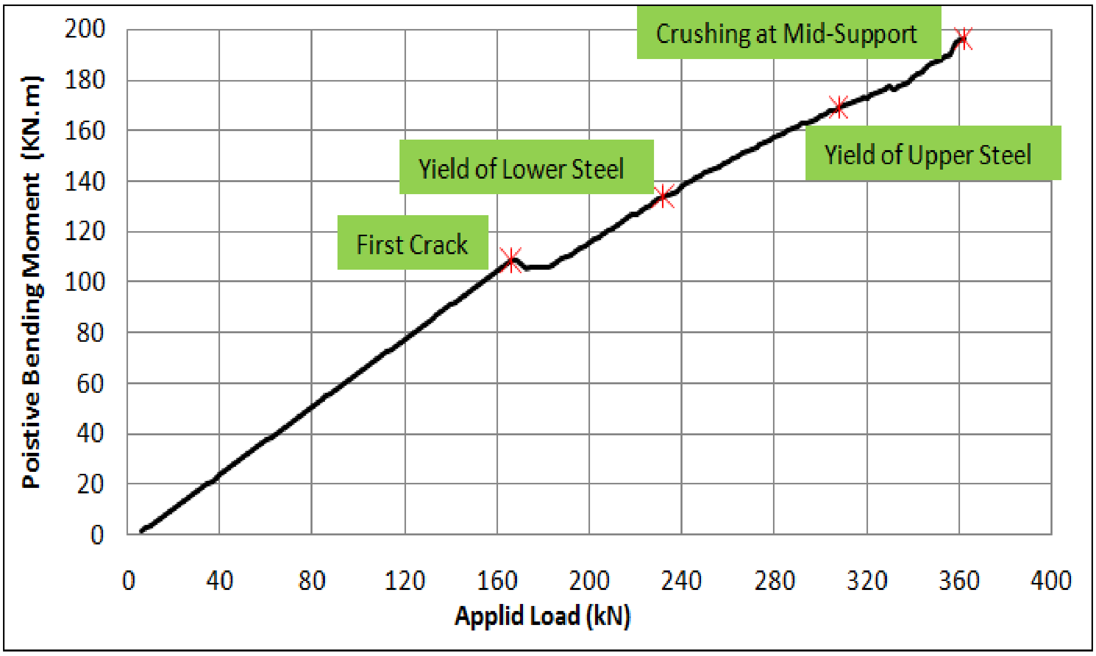


Figure 21. Maximum span moment versus applied loading for strengthened beam

*Debonding Failure Mode*

No additional information was found different from those mentioned in section 4.3.2.
*Rupture Failure Mode*
No rupture occurred in the SMZ since the hogging moment is larger than the sagging one, and hence the CFRP stresses in the span are not high and far away from the value of the CFRP strength.

## Conclusions

This paper examines the different mode failures of RC T-beams strengthened either in the sagging or in the hogging moment zones, using the ANSYS FE Package.
According to the obtained results, the following can be concluded:

- Three types of failure may occur; rupture of the CFRP laminate, debonding of the laminate, and crushing of concrete.

- Rupture occurs, only, if the CFRP stress reaches its maximum value (strength) which occurs when using very small CFRP thickness comparing with the corresponding length.
- Rupture occurs only when strengthening of the HMZ.
- Debonding of CFRP laminates occurs if shear stress, in the adhesive (contact) (bond layer) between the laminate and the concrete, reaches its maximum value.
- Probability of debonding increases with decreasing CFRP length and increasing of CFRP thickness.
- Crushing of concrete occurs as a final stage after yielding of steel reinforcement, formation of a plastic hinge, moment redistribution till the capacity of the beam is reached which means failure.

## References


Saleh A. R. and Barem A. A. H.: Experimental and Theoretical Analysis for Behavior of R.C. Continuous Beams Strengthened by CFRP Laminates. Journal of Babylon University (Iraq) - Engineering Sciences, 21 (5), 1555-1567, (2013).

El-Mogy M., El-Ragaby A., and El-Salakawy E.: Experimental testing and finite element modeling on continuous concrete beams reinforced with fibre reinforced polymer bars and stirrups. Canadian Journal of Civil Engineering, 40 (11), 1091–1102, November, (2013).

El-Refaie S. A., Ashour A. F. and Garrity S. W.: Sagging and Hogging Strengthening of Continuous Reinforced Concrete Beams Using Carbon Fiber-Reinforced Polymer Laminates. ACI Structural Journal, 100 (4), 446-453, July-August, (2003).

Maghsoudi A. A. and Bengar H. A.: Moment redistribution and ductility of RHSC continuous beams strengthened with CFRP. Turkish Journal of Engineering and Environmental Sciences (http://journals.tubitak.gov.tr/engineering/issues/muh-09-33-1/muh-33-1-5-0901-6.pdf), 33, 45-59, (2009).

Saribiyik A. and Caglar N.: Flexural strengthening of RC Beams with low-strength concrete using GFRP and CFRP. Journal of Structural Engineering and Mechanics, 58 (5), 825-845, June, (2016).

Rahman M. M. and Rahman M. W.: Simplified method of strengthening RC continuous T beam in the hogging zone using carbon fiber reinforced polymer laminate - A numerical investigation. Journal of Civil Engineering Construction Technology (http://www.academicjournals.org/JECET), 4 (6), 174-183, June, (2013).

Lu X. Z., Ten J. G., Ye L. P., Jaing J. J.: Bond-slip models for FRP sheets/plates bonded to concrete. Journal of Engineering Structures, 24 (5), 920-937, (2005).

Iesa W. M., Alferjani M. B. S., Ali N. and AbdulSamad A. A.: Study on Shear Strengthening of RC Continuous Beams with Different CFRP Wrapping Schemes. International Journal of Integrated Engineering (Issue on Civil and Environmental Engineering) (http://penerbit.uthm.edu.my/ojs/index.php/ijie/article/view/207), 2 (2), 35-43, (2010).

Aiello M. A. and Ombre, L.: Moment Redistribution in Continuous Fiber-Reinforced Polymer-strengthened Reinforced Concrete Beams. ACI Structural Journal, 158-166, March-April, (2011).

In press article:

Mohie Eldin M., Tarabia A. M. and Hasson R. F.: CFRP Strengthening of Continuous RC T-Beams at Hogging Moment Zone across the Flange. Accepted in Journal of Structural Engineering and Mechanics, Techno-press, 2018 (In Press).

Mohie Eldin M., Tarabia A. M. and Hasson R. F.: Optimum CFRP Length for the Hogging Moment Zone of Continuous RC T-Beams. Accepted in ‘Proceeding of the International Conference on Advances in Civil, Structural and Mechanical Engineering, Antalya, Turkey', October, 2017 (In press).

Books:

Shrestha U. S.: Modified Composite Application to Improve Strength and Ductility of Structural Components. MSc Dissertation, College of Graduate Studies, The University of Toledo, Ohio, United States, (2014).

ANSYS: ANSYS Help. Release 15 (2013).

Book chapters:

Taerwe L., Vasseur L. and Matthys S.: External strengthening of continuous beams with CFRP. in ‘Concrete Repair, Rehabilitation and Retrofitting II’ Alexander et al (eds),Taylor & Francis Group, ISBN 978-0-415-46850-3, London, 43-53, (2009).

Proceedings:

Thorenfeldt E., Tomaszewicz A. and Jensen J.: Mechanical Properties of High Strength Concrete and Application to Design. in ‘Proceedings of the Symposium: Utilization of High-Strength Concrete, Stavanger, Norway’, 149–159, June, (1987).

Sakr M. A., Khalifa T. M. and Mansour W. N.: External Strengthening of RC Continuous Beams Using FRP Plates: Finite Element Model. In ‘Proceeding of the Second International Conference on Advances in Civil, Structural and Mechanical Engineering- CSM 2014’, ISBN: 978-1-63248-054-5, 168-174, (2014).

ECP-203: Egyptian Code of Practice for the Design and Implementation of Reinforced Concrete Structures (2007).

ECP-208: Egyptian Code for the Design Principals and Implementation Requirements of Using CFRP in Fields of Construction (2005).